Correlation energy density from ab initio first- and second-order matrices: a benchmark for approximate functionals.

Süle, P.; Gritsenko, O.V.; Nagy, A.; Baerends, E.J.

published in
Journal of Chemical Physics
1995

DOI (link to publisher)
10.1063/1.469911

document version
Publisher's PDF, also known as Version of record

Correlation energy density from *ab initio* first- and second-order density matrices: A benchmark for approximate functionals

Péter Süle
Institute of Theoretical Physics, Kossuth Lajos University, H-4010 Debrecen, Hungary

Oleg V. Gritsenko
Afdeling Theoretische Chemie, Vrije Universiteit, De Boelelaan 1083, 1081 HV, Amsterdam, The Netherlands

Ágnes Nagy
Institute of Theoretical Physics, Kossuth Lajos University, H-4010 Debrecan, Hungary

Evert Jan Baerends
Afdeling Theoretische Chemie, Vrije Universiteit, De Boelelaan 1083, 1081 HV, Amsterdam, The Netherlands

(Received 21 July 1995; accepted 6 September 1995)

A procedure has been proposed to construct numerically the exchange-correlation $\epsilon_{xc}(\mathbf{r})$ and correlation $\epsilon_c(\mathbf{r})$ energy densities of density functional theory using the correlated first- and second-order density matrices from *ab initio* calculations. $\epsilon_c(\mathbf{r})$ as well as its kinetic and potential components have been obtained for the two-electron He atom and H_2 molecule. The way various correlation effects manifest themselves in the form of $\epsilon_c(\mathbf{r})$ has been studied. The $\epsilon_c(\mathbf{r})$ have been compared with some density functional local and gradient-corrected models $\epsilon_c^{\mathrm{mod}}(\mathbf{r})$. The investigation of the shape of the model energy densities $\epsilon_c^{\mathrm{mod}}(\mathbf{r})$ has been extended to the Be_2 and F_2 molecules and the corresponding correlation energies E_c have been calculated and discussed for a number of atomic and molecular systems. The results show the importance of a proper modeling of $\epsilon_c(\mathbf{r})$ in the molecular bond midpoint region.

I. INTRODUCTION

One of the important advantages of density functional theory (DFT) consists in its efficient treatment of the Coulomb correlation in many-electron systems. The correlation energy functional $E_c[\rho]$ as well as the more general exchange-correlation energy functional $E_{xc}[\rho]$ are represented in DFT with the following integrals:

$$E_{xc}[\rho]=E_x[\rho]+E_c[\rho], \tag{1}$$

$$E_{xc}[\rho]=\int e_{xc}([\rho];\mathbf{r})d\mathbf{r}, \tag{2}$$

$$E_c[\rho]=\int e_c([\rho];\mathbf{r})d\mathbf{r}, \tag{3}$$

$$e_{xc}([\rho];\mathbf{r})=\rho(\mathbf{r})\epsilon_{xc}([\rho];\mathbf{r}), \tag{4}$$

$$e_c([\rho];\mathbf{r})=\rho(\mathbf{r})\epsilon_c([\rho];\mathbf{r}). \tag{5}$$

Here, $E_x[\rho]$ is the exchange energy functional, preferably defined in terms of the Kohn–Sham orbitals, e_{xc} and e_c are the exchange-correlation and correlation energy densities, ϵ_{xc} and ϵ_c are the corresponding energy densities per particle and ρ is the electron density. Modeling of $\epsilon_c([\rho];\mathbf{r})$ with approximate functionals became an essential part of the development of DFT.[1,2]

Usually, approximate functional forms of $\epsilon_c([\rho];\mathbf{r})$ are derived from the homogeneous or inhomogeneous electron gas models[3] with due account of various scaling and asymptotic properties and with the parameters fitted to reproduce E_c values for selected atomic systems. The parameters can also be obtained nonempirically from sum-rule conditions.[4] However, the form of ϵ_c as a function of the electron coordinate $\mathbf{r}$ is seldom taken into consideration and little is still known about the local behavior of the standard ϵ_c models.

A possible reason for this is that Eq. (3) does not define e_c uniquely, since the same E_c value can be obtained with different functionals $e_c(\mathbf{r})$ and $e_c'(\mathbf{r}) = e_c(\mathbf{r}) + f(\mathbf{r})$ whose difference $f(\mathbf{r})$ integrates to zero

$$\int f(\mathbf{r})d\mathbf{r}=0. \tag{6}$$

Nevertheless, in order to perform a consistent analysis of correlation effects and to provide a physically reasonable modeling of ϵ_c, one can choose some suitable definition of $\epsilon_c(\mathbf{r})$ using a particular expression for E_c in terms of a spatial integral over an integrand that is expressed in terms of partially integrated many-electron wave functions. Examples of accurate $\epsilon_c(\mathbf{r})$ obtained in this way for a variety of atoms and molecules, although nonunique, can be helpful for the modeling of accurate $\epsilon_c(\mathbf{r})$.

In this paper a procedure is proposed to construct ϵ_{xc} and ϵ_c numerically using correlated first- and second-order density matrices from *ab initio* calculations. This scheme is applicable to an arbitrary many-electron system, however, in this paper we restrict its application to two-electron systems. $\epsilon_c(\mathbf{r})$ as well as its kinetic $t_c(\mathbf{r})$ and potential $w_c(\mathbf{r})$ components are obtained for the He atom and H_2 molecule (in the latter case for both equilibrium internuclear distance and near-dissociation limit). The corresponding functions $e_c(\mathbf{r})$ are compared with the gradient-dependent models $e_c^{\mathrm{mod}}(\mathbf{r})$ of Perdew and Wang (PW),[5,6] Lee, Yang, and Parr (LYP),[7] Wilson and Levy,[8] and also with some local models.[9,10] To fur-

ther examine the observed trends, the form of $e_c^{\mathrm{mod}}(\mathbf{r})$ is investigated for the Be_2 and F_2 molecules and E_c values are calculated and discussed for a number of atomic and molecular systems.

II. DEFINITION AND CONSTRUCTION OF ϵ_{xc} AND ϵ_c

To define ϵ_{xc} and ϵ_c, we use the following expressions for E_{xc} and E_c:[11]

$$E_{\mathrm{xc}}[\rho]=\frac{1}{2}\int \rho(\mathbf{r})w_{\mathrm{xc}}(\mathbf{r})d\mathbf{r}+\int \rho(\mathbf{r})[v_{\mathrm{kin}}(\mathbf{r}) - v_{s,\mathrm{kin}}(\mathbf{r})]d\mathbf{r}, \tag{7}$$

$$E_c[\rho]=\frac{1}{2}\int \rho(\mathbf{r})w_c(\mathbf{r})d\mathbf{r}+\int \rho(\mathbf{r})[v_{\mathrm{kin}}(\mathbf{r}) - v_{s,\mathrm{kin}}(\mathbf{r})]d\mathbf{r}. \tag{8}$$

The first terms of Eqs. (7) and (8) are the potential contributions to E_{xc} and E_c, with w_{xc} and w_c being potentials of the exchange-correlation and correlation holes, respectively,

$$w_{\mathrm{xc}}(\mathbf{r}_1)=\int \frac{\rho_2^{\lambda=1}(\mathbf{r}_1,\mathbf{r}_2)-\rho(\mathbf{r}_1)\rho(\mathbf{r}_2)}{|\mathbf{r}_1-\mathbf{r}_2|\rho(\mathbf{r}_1)}\,d\mathbf{r}_2 = \int \frac{\rho(\mathbf{r}_2)[g^{\lambda=1}(\mathbf{r}_1,\mathbf{r}_2)-1]}{|\mathbf{r}_1-\mathbf{r}_2|}\,d\mathbf{r}_2, \tag{9}$$

$$w_c(\mathbf{r}_1)=\int \frac{\rho_2^{\lambda=1}(\mathbf{r}_1,\mathbf{r}_2)-\rho_{2s}(\mathbf{r}_1,\mathbf{r}_2)}{|\mathbf{r}_1-\mathbf{r}_2|\rho(\mathbf{r}_1)}\,d\mathbf{r}_2 = \int \frac{\rho(\mathbf{r}_2)[g^{\lambda=1}(\mathbf{r}_1,\mathbf{r}_2)-g_s(\mathbf{r}_1,\mathbf{r}_2)]}{|\mathbf{r}_1-\mathbf{r}_2|}\,d\mathbf{r}_2. \tag{10}$$

In Eqs. (9) and (10) $\rho_2^{\lambda=1}(\mathbf{r}_1,\mathbf{r}_2)$ and $g^{\lambda=1}(\mathbf{r}_1,\mathbf{r}_2)$ are the diagonal part of the second-order density matrix and the pair-correlation function with the electron interaction λ/r_{12} at full strength, $\lambda=1$, while $\rho_{2s}(\mathbf{r}_1,\mathbf{r}_2)$ and $g_s(\mathbf{r}_1,\mathbf{r}_2)$ correspond to $\lambda=0$, i.e., the one-determinantal wave function Ψ_s built from the Kohn–Sham orbitals $\phi_i(\mathbf{r})$

$$\rho_{2s}(\mathbf{r}_1,\mathbf{r}_2)=\rho(\mathbf{r}_1)\rho(\mathbf{r}_2)-\frac{1}{2}\sum_{i=1}^{N}\sum_{j=1}^{N}\phi_i(\mathbf{r}_1)\phi_i^*(\mathbf{r}_2) \times\phi_j^*(\mathbf{r}_1)\phi_j(\mathbf{r}_2). \tag{11}$$

$w_c(\mathbf{r})$ represents the potential of the full exchange-correlation hole density minus the exchange-only hole density of the Kohn–Sham determinant, i.e., the potential of the Coulomb hole.

Equations (7) and (8) have the same second term, which is the kinetic contribution to E_c with the local potential $v_{\mathrm{kin}}(\mathbf{r})$ being defined as follows:[12]

$$v_{\mathrm{kin}}(\mathbf{r}_1)=\frac{1}{2}\int |\nabla_1\Phi(s_1,\mathbf{x}_2,\ldots,\mathbf{x}_N|\mathbf{r}_1)|^2 ds_1\, d\mathbf{x}_2\cdots d\mathbf{x}_N = \frac{\nabla_{1'}\nabla_1\rho^{\lambda=1}(\mathbf{r}_1',\mathbf{r}_1)|_{\mathbf{r}_{1'}=\mathbf{r}_1}}{2\rho(\mathbf{r}_1)}-\frac{[\nabla\rho(\mathbf{r}_1)]^2}{8\rho^2(\mathbf{r}_1)}. \tag{12}$$

In Eq. (12) $\Phi(s_1,\mathbf{x}_2,\ldots,\mathbf{x}_N|\mathbf{r}_1)$ is the conditional probability amplitude[13] of the total wave function $\Psi(\mathbf{x}_1,\mathbf{x}_2,\ldots,\mathbf{x}_N)$ ($\{\mathbf{x}_i\}=\{\mathbf{r}_i,s_i\}$, $\{\mathbf{r}_i\}$ are the space and $\{s_i\}$ are the spin variables)

$$\Phi(s_1,\mathbf{x}_2,\ldots,\mathbf{x}_N|\mathbf{r}_1)=\frac{\Psi(\mathbf{x}_1,\ldots,\mathbf{x}_N)}{\sqrt{\rho(\mathbf{r}_1)/N}} \tag{13}$$

and $\rho^{\lambda=1}(\mathbf{r}_1',\mathbf{r}_1)$ is the first-order density matrix for $\lambda=1$. $\Phi(s_1,\mathbf{x}_2,\ldots,\mathbf{x}_N|\mathbf{r}_1)$ embodies all effects of electron correlation (exchange as well as Coulomb) in that its square is the probability distribution of the remaining $N-1$ electrons associated with positions $\mathbf{x}_2,\ldots,\mathbf{x}_N$ when one electron is known to be at $\mathbf{r}_1$. v_{kin} can be interpreted as a measure of how strongly the motion of the reference electron at $\mathbf{r}_1$ is correlated with other electrons in the system, in the sense that it reflects the magnitude of change in Φ with changing $\mathbf{r}_1$ (so it is a measure of the *change* in correlation hole with reference position $\mathbf{r}_1$). $v_{s,\mathrm{kin}}$ is defined analogously to v_{kin} in terms of the Kohn–Sham functions

$$v_{s,\mathrm{kin}}(\mathbf{r}_1)=\frac{1}{2}\int |\nabla_1\Phi_s(s_1,\mathbf{x}_2,\ldots,\mathbf{x}_N|\mathbf{r}_1)|^2\, ds_1\, d\mathbf{x}_2\cdots d\mathbf{x}_N = \frac{1}{2}\sum_{i=1}^{N}\left|\nabla_1\frac{\phi_i(\mathbf{r}_1)}{\rho^{1/2}(\mathbf{r}_1)}\right|^2, \tag{14}$$

$$\Phi_s(s_1,\mathbf{x}_2,\ldots,\mathbf{x}_N|\mathbf{r}_1)=\frac{\Psi_s(\mathbf{x}_1,\ldots,\mathbf{x}_N)}{\sqrt{\rho(\mathbf{r}_1)/N}}. \tag{15}$$

From Eqs. (7) and (8) one can define ϵ_{xc} and ϵ_c as follows:

$$\epsilon_{\mathrm{xc}}(\mathbf{r})=\tfrac{1}{2}w_{\mathrm{xc}}(\mathbf{r})+v_{\mathrm{kin}}(\mathbf{r})-v_{s,\mathrm{kin}}(\mathbf{r}), \tag{16}$$

$$\epsilon_c(\mathbf{r})=\tfrac{1}{2}w_c(\mathbf{r})+v_{\mathrm{kin}}(\mathbf{r})-v_{s,\mathrm{kin}}(\mathbf{r}). \tag{17}$$

Note, that in DFT alternative definitions of ϵ_{xc} and ϵ_c are often used, in which they are expressed via integrals over the coupling parameter λ[14,15]

$$\epsilon_{\mathrm{xc}}(\mathbf{r}_1)=\frac{1}{2}\int\int_0^1 \frac{\rho(\mathbf{r}_2)[g^{\lambda}(\mathbf{r}_1,\mathbf{r}_2)-1]}{|\mathbf{r}_1-\mathbf{r}_2|}\,d\lambda\, d\mathbf{r}_2, \tag{18}$$

$$\epsilon_c(\mathbf{r}_1)=\frac{1}{2}\int\int_0^1 \frac{\rho(\mathbf{r}_2)[g^{\lambda}(\mathbf{r}_1,\mathbf{r}_2)-g_s(\mathbf{r}_1,\mathbf{r}_2)]}{|\mathbf{r}_1-\mathbf{r}_2|}\,d\lambda\, d\mathbf{r}_2. \tag{19}$$

In this paper, however, we choose definitions (16) and (17) as more convenient ones for our purpose. Having available functions $\rho(\mathbf{r}_1),\rho(\mathbf{r}_1',\mathbf{r}_1),\rho_2(\mathbf{r}_1,\mathbf{r}_2),\{\phi_i(\mathbf{r}_1)\}$ for a real system with $\lambda=1$, one can calculate ϵ_{xc} and ϵ_c via Eqs. (16) and (17), so knowledge concerning the dependence on λ is not needed.

Bearing this in mind, we propose to construct $\epsilon_{\mathrm{xc}}(\mathbf{r})$ and $\epsilon_c(\mathbf{r})$ as well as the exchange-correlation Kohn–Sham potential $v_{\mathrm{xc}}(\mathbf{r})$ numerically by a combined procedure from the correlated first- and second-order density matrices obtained with *ab initio* calculations. This procedure is based on recently proposed methods[16–18] to construct $v_{\mathrm{xc}}(\mathbf{r})$ and $\{\phi_i(\mathbf{r})\}$ from $\rho(\mathbf{r})$ for general atomic and molecular systems (cf. also Refs. 19–23 for earlier v_{xc} determinations/proposals). The procedure consists of the following steps:

(1) A set $\{\phi_i(\mathbf{r})\}$ and $v_{\rm xc}(\mathbf{r})$ are obtained from the correlated $\rho(\mathbf{r})$ using one of the above-mentioned methods. We use the simple and efficient method of Ref. 17 (a similar method has been developed in Ref. 16), which has recently been successfully applied to molecules.[24]
(2) $v_{\rm kin}(\mathbf{r})$ is calculated from correlated $\rho(\mathbf{r}',\mathbf{r})$ via Eq. (12) and $w_{\rm xc}(\mathbf{r})$ is calculated from $\rho(\mathbf{r})$ and $\rho_2(\mathbf{r}_1,\mathbf{r}_2)$ via Eq. (9).
(3) $v_{s,\rm kin}(\mathbf{r})$ is calculated from $\{\phi_i(\mathbf{r})\}$ and $\rho(\mathbf{r})$ via Eq. (14) and $w_c(\mathbf{r})$ is calculated from $w_{\rm xc}(\mathbf{r})$ and $\{\phi_i(\mathbf{r})\}$ via Eqs. (9)–(11).
(4) The energy densities $\epsilon_{\rm xc}(\mathbf{r}),\epsilon_c(\mathbf{r}),e_{\rm xc}(\mathbf{r}),e_c(\mathbf{r})$ are obtained according to Eqs. (4), (5), (16), and (17).

For two-electron systems this procedure is essentially simplified, since in this case there is only one occupied Kohn–Sham orbital $\phi_1(\mathbf{r})$, equal (up to a phase factor) to $\rho^{1/2}(\mathbf{r})/\sqrt{2}$. Therefore, the first step of the procedure is effectively eliminated and $\epsilon_{\rm xc}(\mathbf{r}),\epsilon_c(\mathbf{r})$ can be calculated directly from $\rho(\mathbf{r}',\mathbf{r})$ and $\rho_2(\mathbf{r}_1,\mathbf{r}_2)$. In particular, by definition (14), $v_{s,\rm kin}$ vanishes for a two-electron system, so that $\epsilon_c(\mathbf{r})$ turns into

$$\epsilon_c(\mathbf{r})=\tfrac{1}{2}w_c(\mathbf{r})+v_{\rm kin}(\mathbf{r}). \tag{20}$$

Exchange in this case reduces to a pure electron self-interaction and $w_c(\mathbf{r})$ transforms into

$$w_c(\mathbf{r}_1)=\int \frac{\rho(\mathbf{r}_2)[g^{\lambda=1}(\mathbf{r}_1,\mathbf{r}_2)-\frac{1}{2}]}{|\mathbf{r}_1-\mathbf{r}_2|}\,d\mathbf{r}_2. \tag{21}$$

Function (20) contains interesting information about the local effect of the Coulomb correlation of two electrons with opposite spins.

In this paper $\epsilon_c(\mathbf{r})$ [with its kinetic $v_{\rm kin}(\mathbf{r})$ and potential $(1/2)w_c(\mathbf{r})$ components] and $e_c(\mathbf{r})$ are obtained for the two-electron He atom and H_2 molecule in order to study the local effect of correlation in these simple cases and to provide the first example of accurate correlation energy densities calculated from correlated wave functions. These functions has been obtained from full configuration interaction (CI) calculations of the ground states of He and H_2 in a basis of contracted Gaussian functions. For He the basis has been used, which was obtained in Refs. 12 and 25 by expansion of the Slater-type functions of a $5s,4p,3d$ basis[26] in six Gaussians (STF-6GF). CI calculation in this basis yields $E_c=-0.041$ a.u., i.e., more than 97% of the correlation energy is recovered for He.

For the H_2 molecule calculations have been performed at the equilibrium distance $R(\mathrm{H–H})=1.401$ a.u. and also in the near-dissociation limit at $R(\mathrm{H–H})=5.0$ a.u. A basis with five s- and two p-type functions[27,28] and an extra d-type Gaussian with the exponent $\alpha=1.0$ has been used for the H atoms. In this basis $E_c=-0.039$ a.u. has been obtained for the equilibrium distance, which corresponds to more than 95% of the correlation energy. Calculation of $\rho(\mathbf{r}',\mathbf{r})$ and $\rho_2(\mathbf{r}_1,\mathbf{r}_2)$ from the full CI wave functions with the subsequent construction of $v_{\rm kin}(\mathbf{r})$ and $w_c(\mathbf{r})$ has been performed with a specialized density functional extension[12,25] of the *ab initio* ATMOL package.[29] The functions $\epsilon_c(\mathbf{r})$ and $e_c(\mathbf{r})$ thus obtained will be presented and compared with the corresponding local and gradient-dependent models in the next sections.

III. MODEL FUNCTIONALS $\epsilon_c([\rho];\mathbf{r})$

The model functionals $\epsilon_c([\rho];\mathbf{r})$ to be compared here with each other and with those obtained from *ab initio* calculations are the local density approximation (LDA) in the parameterization of Perdew and Wang,[10] the local Wigner (LW) function[30] and the gradient-dependent PW,[5,6] LYP,[7] and WL[8] models. The LDA function $\epsilon_c^{\rm LDA}(r_s)$[10] represents the dependence of the correlation energy density per electron of the homogeneous electron gas model[3] on the Wigner radius r_s

$$r_s=\left[\frac{3}{4\pi\rho}\right]^{1/3} \tag{22}$$

in a wide range of densities (here we consider closed-shell systems with the spin-polarization parameter ζ being equal to zero). $\epsilon_c^{\rm LDA}(r_s)$ interpolates between the logarithmic dependence on r_s in the high-density limit[31] and the inverse-power dependence on r_s in the low-density limit (the Wigner crystal).[30]

The PW model $\epsilon_c^{\rm PW}(r_s,\nabla\rho(\mathbf{r}))$[5,6] is the gradient extension of the LDA

$$\epsilon_c^{\rm PW}(r_s,\nabla\rho(\mathbf{r}))=\epsilon_c^{\rm LDA}(r_s)+H(r_s,\nabla\rho(\mathbf{r})) \tag{23}$$

with the correction term $H(r_s,\nabla\rho(\mathbf{r}))$ being, essentially, a logarithmic function of the Padé approximant of the argument t

$$t=c\,\frac{|\nabla\rho(\mathbf{r})|\sqrt{r_s}}{\rho(\mathbf{r})}. \tag{24}$$

The parameters of $H(r_s,\nabla\rho(\mathbf{r}))$ were fitted to reproduce integral (19) of the model correlation hole, the latter being obtained with the real space cut off of the correlation hole function of the second-order gradient expansion approximation (GEA).[4]

The rest of the model functionals to be considered can be defined as Wigner-like functionals, which are represented with the following formula:

$$\epsilon_c^{\rm mod}([\rho];\mathbf{r})=\frac{a}{c+f_1(\rho(\mathbf{r}),\nabla\rho(\mathbf{r}))+r_s+f_2(\rho(\mathbf{r}),\nabla\rho(\mathbf{r}))}. \tag{25}$$

In the simplest case $f_1=f_2=0$ and Eq. (25) reduces to the LW function,[30] which interpolates between the inverse dependence on r_s in the low-density limit and the typical correlation energy per electron for a certain type of systems for higher densities. Various modifications of the LW function were proposed in the literature with the parameters determined to reproduce correlation of the valence electrons in metals[9] or E_c values of certain atoms.[32] In this paper we use the LW function with the parameters $a=-0.027\,28$ and $c=0.218\,82$, which have been fitted in Ref. 33 to reproduce the conventional E_c values[34] of eight closed-shell atomic systems He, Li^+, Be^{2+}, Be, B^+, Ne, Mg, Ar.

With f_1 and f_2 of the following form:

$$f_1(\rho(\mathbf{r}),\nabla\rho(\mathbf{r}))=d\,\frac{|\nabla\rho(\mathbf{r})|}{\left(\frac{\rho(\mathbf{r})}{2}\right)^{4/3}}, \tag{26}$$

$$f_2(\rho(\mathbf{r}),\nabla\rho(\mathbf{r}))=b\,\frac{|\nabla\rho(\mathbf{r})|}{\rho^{4/3}(\mathbf{r})[c+f_1(\rho(\mathbf{r}),\nabla\rho(\mathbf{r}))+r_s]}, \tag{27}$$

formula (25) defines the Wilson–Levy (WL) functional.[8] Its parameters were fitted to reproduce the E_c value for He and the scaling relations for the E_c functional[35] for the eight above-mentioned atomic systems.

With $f_1=0$ and f_2 being a rather lengthy function of $\rho(\mathbf{r})$ and $\nabla\rho(\mathbf{r})$ (so we do not present it in the text) formula (25) defines the Lee–Yang–Parr (LYP) functional.[7] It was derived as the second-order gradient expansion of the Colle–Salvetti formula,[36] in which originally a parameter was fitted to reproduce the E_c value for the He atom. We use the gradient-only representation of the LYP functional, which was obtained in Ref. 37 by partial integration.

In order to make a consistent comparison and in accordance with the original formulation of the LYP and WL functionals, the Hartree–Fock (HF) densities $\rho^{\mathrm{HF}}(\mathbf{r})$ have been used to calculate the model functionals $e_c^{\mathrm{mod}}([\rho];\mathbf{r})$ and correlation energies E_c for atoms and molecules, except for H_2 at $R=5.0$ bohr, where the HF density differs strongly from the exact density and the Kohn–Sham orbital differs strongly from the HF orbital.[38] HF calculations have been performed with the GAMESS program package[39] in a triple zeta Gaussian basis set with additional $3d$-polarization functions (Dunning's TZVP basis[40,41]). $e_c^{\mathrm{mod}}([\rho];\mathbf{r})$ and E_c have been calculated from the HF wave functions with the density functional program DETEDF.[33] A numerical integration by the Monte Carlo method[42] has been used to obtain E_c values. The corresponding results will be presented and discussed in the next sections.

IV. RESULTS FOR ATOMS

Figure 1 displays $\epsilon_c(r)$ (r is the atomic radial coordinate) as well as its potential $\frac{1}{2}w_c(r)$ and kinetic $v_{\mathrm{kin}}(r)$ components obtained from the full CI functions $\rho(\mathbf{r}',\mathbf{r})$ and $\rho_2(\mathbf{r}_1,\mathbf{r}_2)$ for the He atom. The form of $\epsilon_c(r)$ is determined primarily by that of its potential component. Both ϵ_c and w_c are everywhere negative functions, while v_{kin} is everywhere positive. Both ϵ_c and w_c are monotonous functions of r with their minima at the nucleus due to strong in–out correlation of the reference electron at $r=0$. Contrary to this, v_{kin} is a rather shallow nonmonotonous function with a maximum that is placed near that of the radial density $r^2\rho(r)$. Near the nucleus v_{kin} goes closer to zero (note the exact asymptotics $v_{s,\mathrm{kin}}(r\downarrow 0)=0$ of the Kohn–Sham kinetic potential in this case.[11,12]

In Fig. 2 $e_c(r)$ obtained from the CI calculations and the the corresponding radial function $4\pi r^2 e_c(r)$ are compared with those of PW, LYP, WL, and LW models. The various functions e_c appear to have quite different local behaviors. In particular, e_c^{LYP} and e_c^{LW} have a rather shallow form in the inner region $r<0.3$ a.u. [see Fig. 2(a)], while e_c, e_c^{PW}, and e_c^{WL} are appreciably more sharp functions of r. In this inner region the w_c contribution dominates, which is just the potential of the Coulomb hole [cf. Eq. (10)]. It is known that the Coulomb hole in this region represents mostly in–out correlation, being negative around the nucleus and the position of the reference electron and becoming positive much further outwards.[38] The resulting negative w_c and ϵ_c in this region are clearly underestimated by all model functionals (except for the nuclear peak of ϵ_c^{WL} which has no energetic effect due to the vanishingly small volume). At larger r values, i.e., r in the region 0.5–1.4 a.u., where the Coulomb hole has a characteristic polarization shape,[38] all the model energy densities $\epsilon_c^{\mathrm{mod}}$ are larger (i.e., more negative) than ϵ_c, as is clearly visible in Fig. 2(b), where the radial weight factor $4\pi r^2$ makes this property stand out more clearly. All the radial functions corresponding to model energy densities have their maxima around $r=0.5$ a.u., while the maximum in e_c occurs at somewhat shorter r (ca. 0.3). The PW, LYP, and WL radial functions have rather similar behavior in the region $r<1.25$ a.u., while the LW function is more diffuse and the exact $4\pi r^2 e_c(r)$ is relatively more contracted [see Fig. 2(b)]. It is evident from the shape of the various model $4\pi r^2 e_c^{\mathrm{mod}}$ that they may integrate to an E_c value close to the one obtained from the exact e_c since the underestimation for r values below ca. 0.4 a.u. will be compensated by the overestimation for larger r. Indeed, parameters in all of the model e_c^{mod}'s except PW have been adapted to achieve this exactly or approximately.

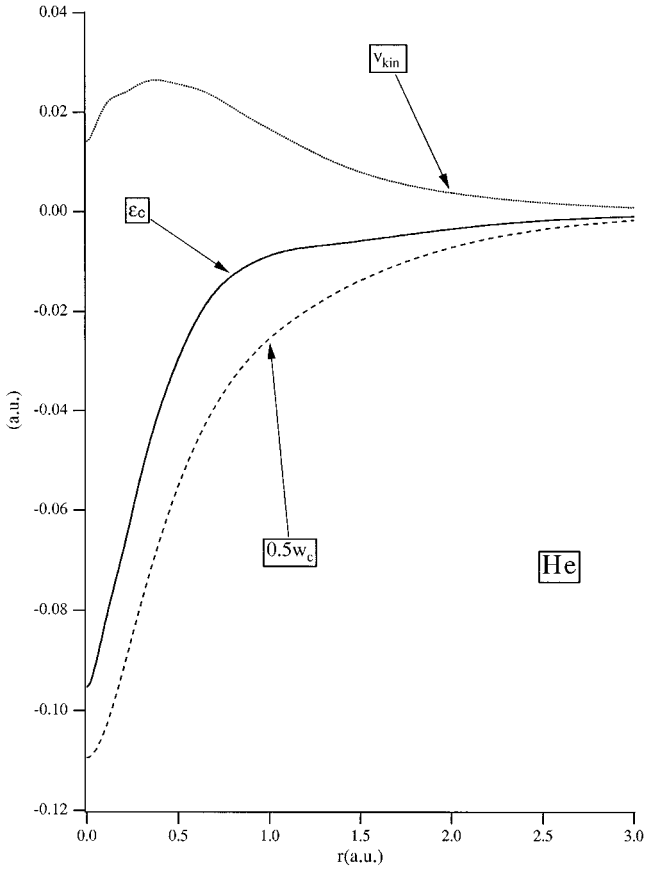

FIG. 1. Correlation energy density $\epsilon_c(r)$ and its components $0.5w_c(r)$ and $v_{\mathrm{kin}}(r)$ for He.

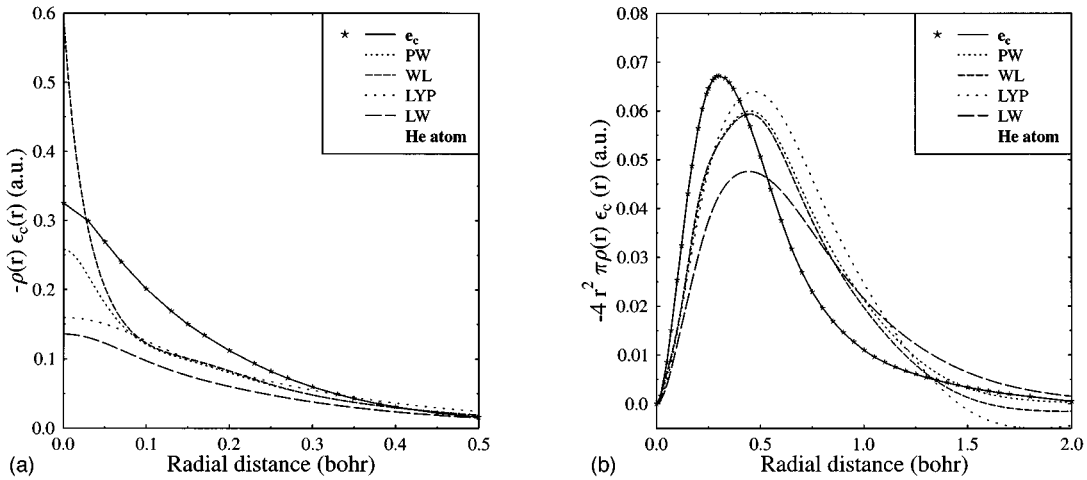

FIG. 2. Correlation energy density $e_c(r)$ and model functionals $e_c^{\mathrm{mod}}(r)$ for He.

Table I represents E_c values for 13 closed-shell atomic systems calculated with the model functionals $\epsilon_c^{\mathrm{mod}}(\mathbf{r})$. In spite of the above-mentioned differences in the local behavior, all models yield for He E_c values which are close to the conventional $E_c=-0.042$ a.u. [to be more precise, one should mention a slight overestimation $E_c=-0.046$ a.u. of the (nonempirical) PW model]. The only exception is the LDA, which is not presented in Figs. 1 nor 2 but is included in Table I.

The same trend holds in the general case of neutral atoms. LDA yields E_c values which are about twice as large (in absolute magnitude) as the conventional ones and E_c values of other models. This well-known feature of the LDA originates from the difference in correlation between the extended homogeneous electron gas model (which is represented by the LDA) and finite inhomogeneous atomic systems.[43] For the former system the Coulomb correlation of electrons with like spins brings about the same contribution to E_c as that of the opposite-spin electrons. However, in finite atomic systems correlation of like-spin electrons is substantially suppressed by their exchange, so that it brings a small contribution to E_c.

All other models considered yield rather close E_c values for neutral atomic systems, which agree satisfactorily with the available empirical data. One can only mention some relative underestimation of correlation for heavier atoms in the LYP model (see Table I). As a matter of fact, the least deviation from the conventional E_c values is achieved in the WL model. On the other hand, one should note the success of the PW model, which without empirical parameters manages to describe adequately both the homogeneous electron gas (as its zero-gradient limit) and atoms.

For ionic systems the picture is less consistent. WL, LYP and, to a lesser extent, PW reproduce the conventional E_c values for the two-electron Li^+ and Be^{2+} systems, while they fail to reproduce it for the four-electron Ne^{6+}. However, the opposite trend is observed for the LW model. All functionals fail to reproduce accurately the E_c value for the F^- anion.

To sum up, the results obtained illustrate a somewhat confused situation for the atomic applications of various ϵ_c models. In spite of their different functional form and local behavior, a number of $\epsilon_c^{\mathrm{mod}}$ functions yield rather close-lying satisfactory E_c values. From the particular case of the He atom discussed above (see Fig. 2) one can assume that also for the general case there will be considerable local differences amongst the $\epsilon_c^{\mathrm{mod}}(r)$, and between the $\epsilon_c^{\mathrm{mod}}(r)$ and the exact $\epsilon_c(r)$, in the inner region as well as at large distances. As the differences in these regions have opposite sign, they do not affect the E_c values due to cancellation. As has been demonstrated in this section all the $\epsilon_c^{\mathrm{mod}}$, in spite of their differences (more diffuse or more contracted towards the nucleus; all more diffuse than e_c) can produce satisfactory overall E_c values. Unfortunately, as will be shown in the next section, the molecular performance of ϵ_c models is not so satisfactory.

TABLE I. Correlation energies of atoms obtained by various approximate correlation energy functionals.[a]

	WL	LYP	PW	LW	LDA	EXP
He	0.042	0.043	0.046	0.042	0.112	0.042
Be	0.094	0.094	0.094	0.094	0.223	0.094
Ne	0.383	0.383	0.383	0.374	0.743	0.392
Mg	0.444	0.459	0.451	0.462	0.888	0.444
Ar	0.788	0.750	0.771	0.771	1.426	0.787
Kr	1.909	1.748	1.916	1.948	3.267	
Xe	3.156	2.742	3.150	3.174	5.173	
Li^+	0.044	0.047	0.051	0.060	0.134	0.044
Be^{2+}	0.045	0.049	0.053	0.075	0.150	0.044
Ne^{6+}	0.109	0.129	0.123	0.187	0.334	0.187
B^+	0.101	0.106	0.103	0.114	0.252	0.111
Li^-	0.0805	0.0732	0.078	0.069	0.182	0.073
F^-	0.368	0.362	0.362	0.332	0.696	0.400

[a]WL, LYP, PW, LW, LDA, and EXP denotes Wilson–Levy functional (Ref. 8), Lee–Yang–Parr functional (Ref. 7), Perdew and Wang *gradient corrected* functional (Refs. 4, 10), local Wigner functional (Refs. 30, 33), Perdew and Wang *local* correlation functional (Ref. 5). EXP denotes the experimental correlation energies. [A. Savin, H. Stoll, and H. Preuss, Theor. Chim. Acta. **70**, 407 (1986)], respectively. For Ne and Ne^{6+} we used the more accurate values from the following reference: E. R. Davidson, S. A. Hagstrom, and S. J. Chakravorty, Phys. Rev. A **44**, 7071 (1991). All the energies are in a.u. The calculations were performed using the large TZV+3D basis.

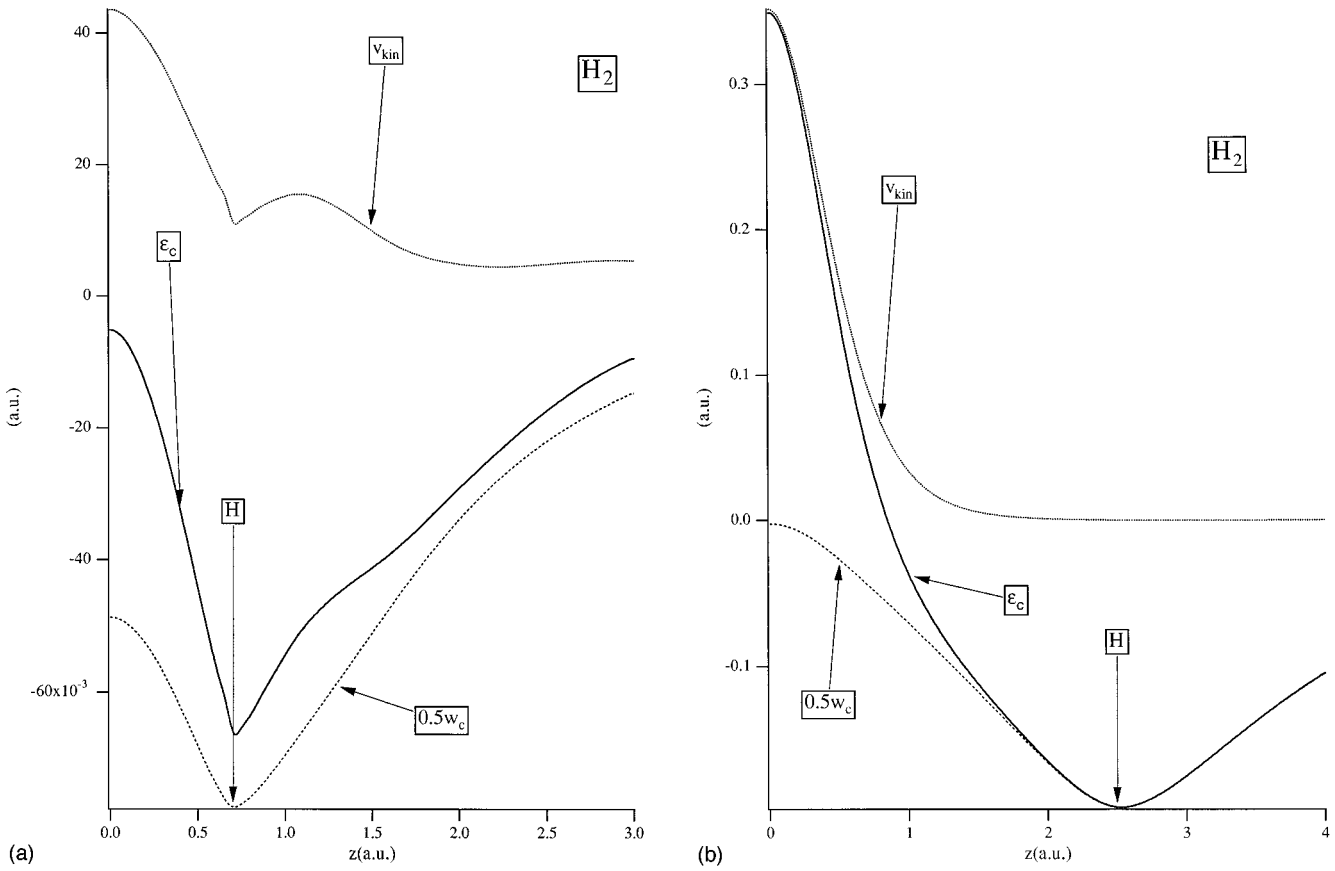

FIG. 3. Correlation energy density $\epsilon_c(z)$ and its components $0.5w_c(z)$ and $e_{\rm kin}(z)$ for H_2 at equilibrium distance (a) and near dissociation limit (b) along the bonding axis. The bond midpoint is at $z=0.0$ and hydrogen atomic position is at $z=0.7$ (a) or $z=2.5$ a.u. (b).

V. RESULTS FOR MOLECULES

In Fig. 3 ϵ_c for H_2 is presented as the first example of a molecular correlation energy density obtained from the correlated *ab initio* $\rho(\mathbf{r}',\mathbf{r})$ and $\rho_2(\mathbf{r}_1,\mathbf{r}_2)$. ϵ_c as well as its potential $(1/2)w_c$ and kinetic $v_{\rm kin}$ components are plotted for both equilibrium internuclear distance $R(\text{H–H})=1.401$ a.u. [Fig. 3(a)] and for large distance $R(\text{H–H})=5.0$ a.u. along the bond axis as a function of the distance z from the bond midpoint. [$v_{\rm kin}$ and w_c $(=V^{\rm cond}-V^{\rm HF})$ individually have been calculated before; see Ref. 12.]

The form of w_c, $v_{\rm kin}$, and ϵ_c reflects the left–right electron correlation, the dominating correlation effect in H_2. The notion of the left–right correlation implies that if the reference electron is in the neighborhood of the H nucleus, there is a large probability for the other electron to be in the neighborhood of the other H nucleus. Left–right correlation is greatly amplified in the dissociation limit due to the strong near-degeneracy effects.

The most noticeable features in Fig. 3 are the wells of $w_c(z)$ and $\epsilon_c(z)$ around the nucleus and the peaks of $v_{\rm kin}(z)$ and $\epsilon_c(z)$ at the bond midpoint. The well of $w_c(z)$ with the minimum at the H nucleus reflects the appreciable reduction of the electron–electron repulsion in this region due to the left–right correlation. w_c is the Coulomb hole potential [see Eq. (10)] and is also a part of $v_{\rm xc}$ (together with the potential from the Fermi hole it constitutes the total hole potential, which is an important part of $v_{\rm xc}$). The attractive nature of w_c will have the effect of making the density more compact around the H nuclei, which is precisely what is required in view of the much too diffuse density that results in an exchange-only treatment.[12] Closer to the bond midpoint, the left–right correlation becomes less important and $w_c(z)$ is closer to zero. Having the same qualitative features, the functions $w_c(z)$ for the equilibrium and large H–H distances differ quantitatively. The minimum of $w_c(z)$ for $R(\text{H–H})=5.0$ a.u. is about twice as deep as that for $R(\text{H–H})=1.401$, in accordance with the stronger near-degeneracy left–right correlation at large distance. On the other hand, the local maximum of $w_c(z)$ at the bond midpoint is much closer to zero for $R(\text{H–H})=5.0$. Indeed, when the reference electron is at the bond midpoint, which is in this case a region of very low density, we may expect hardly any Coulomb hole, since the symmetrical exchange hole of depth $-\rho(\mathbf{r})/2$ will in this case already be a good description of the total exchange-correlation hole.

Left–right correlation finds a spectacular way to manifest itself through the bond midpoint peak of $v_{\rm kin}(z)$.[12] By definition (12), $v_{\rm kin}(\mathbf{r})$ is determined by the average rate of change of the conditional amplitude $\Phi(s_1,\mathbf{x}_2,\ldots,\mathbf{x}_N|\mathbf{r}_1)$ with changing position $\mathbf{r}_1$ of the reference electron. Φ has the maximal gradient at the bond midpoint $z=0$, since when the reference electron crosses the bond midpoint, the other electron has to switch quickly from one atom to another due to the left–right correlation. As a consequence, $v_{\rm kin}(z)$ pos-

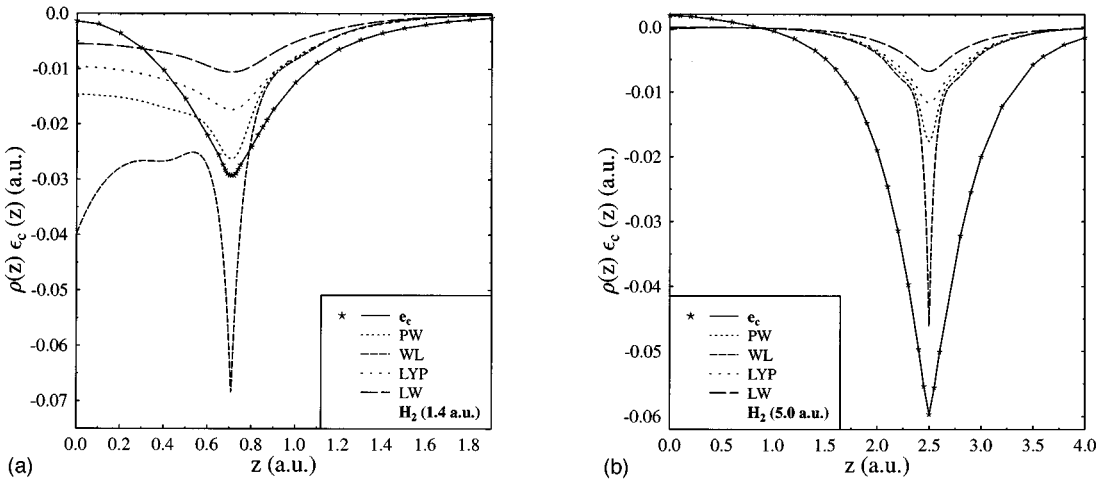

FIG. 4. Correlation energy density $e_c(z)$ and models $e_c^{\mathrm{mod}}(z)$ for H_2 at equilibrium distance (a) and near dissociation limit (b) along the bonding axis.

sesses a peak at $z=0$, which reflects the corresponding ''jump'' of the conditional amplitude. This peak becomes much higher for large H–H distance, because of increase of left–right correlation in the dissociation limit. We can also mention the nonmonotonous behavior of $v_{\mathrm{kin}}(z)$ in Fig. 3(a), with a local minimum at the H nucleus. The exact v_{kin} is not necessarily zero at the nucleus in this case, but clearly still exhibits this tendency.

The above-mentioned individual features of $w_c(z)$ and $v_{\mathrm{kin}}(z)$ can be clearly recognized in the plots of the resulting $\epsilon_c(z)$. This is especially true for $R(\mathrm{H–H})=5.0$ a.u. [see Fig. 3(b)]. In this case $\epsilon_c(z)$ inherits the bond midpoint peak of $v_{\mathrm{kin}}(z)$ and the well around the nucleus of $(1/2)w_c(z)$, with the height of the peak and the depth of the well being very close to those for v_{kin} and $(1/2)w_c$. Because of this, ϵ_c becomes a sign-changing function: It is positive in the bond midpoint region, it changes sign near $z=1$ a.u.; and it is negative at larger z. For the equilibrium geometry, on the other hand, $\epsilon_c(z)$ is everywhere negative [see Fig. 3(a)]. In this case both $(1/2)w_c(z)$ and $v_{\mathrm{kin}}(z)$ have appreciable contributions to $\epsilon_c(z)$ at all z considered. Still, ϵ_c has the same qualitative features, namely, a maximum at the bond midpoint and a well around the H nucleus.

In Fig. 4 $e_c(z)$ obtained for H_2 from *ab initio* $\rho(\mathbf{r}',\mathbf{r})$ and $\rho_2(\mathbf{r}_1,\mathbf{r}_2)$ is compared with those of the PW, LYP, WL, and LW models. As has been mentioned in Sec. III, the gradient models were parametrized from atomic data (LYP, WL) or obtained from the GEA for the inhomogeneous electron gas model with suitable cutoffs (PW). However, as regards the density gradients, there is a basic difference between atoms and molecules. For atoms $|\nabla\rho(\mathbf{r})|$ is never small, while for molecules it is close to zero in the important bond midpoint region. One can expect also, that correlation effects in this molecular region differ from those in the homogeneous or weakly inhomogeneous electron gas models. Because of this, $e_c^{\mathrm{mod}}(\mathbf{r})$ may have rather accidental behavior in the bond midpoint region. Therefore, it is interesting to investigate the form of the model $e_c^{\mathrm{mod}}(z)$ and compare them with that of the exact $e_c(z)$ which, as has been shown for the corresponding function $\epsilon_c(z)$, embodies in a transparent manner the effects of correlation.

Considering first the bond region, Fig. 4(a) shows a rather different behavior of the various energy density functions in the region between the nuclei for the equilibrium H–H distance. In complete analogy with $\epsilon_c(z)$, the characteristic feature of $e_c(z)$ in this region is the maximum (close to zero) at the bond midpoint. The PW, LYP, and LW models also have maxima at the bond midpoint, however, they are considerably more shallow functions of z than is $e_c(z)$. On the other hand, the Wilson–Levy energy density $e_c^{\mathrm{WL}}(z)$ is a much more negative function in the bond region, exhibiting a sharp minimum at $z=0$. This minimum seems to be an artifact of the WL function and it will appear for an arbitrary molecular system as a consequence of the functional form of the WL model [Eqs. (25)–(27)] and the relation $d \gg b$ between the parameters of this model.

Near the nuclei the various model energy density functions are similar to those found for the He atom [compare Figs. 2(a) and 4(a)], as may be expected from their dependence on the density. The wells of the exact e_c around the nuclei are also reminiscent of the shape of e_c in He, but it should be noted that the underlying correlation is very different: The Coulomb hole is now due to left–right correlation rather than to in–out correlation. This difference becomes manifest in the outer tail. Whereas in He the model energy densities become more negative than e_c at distances from the nucleus larger than ca. 0.4 a.u., in H_2 e_c remains more negative in the complete tail region [see Fig. 4(a) for large values of z]. This may be understood from the strong left–right correlation that will be present when the reference electron is at these positions. This difference in the physics of the correlation compared to He is clearly not recognized by the model correlation functionals. Obviously, there will again be compensation of errors, the model functionals giving more negative contributions around the bond midpoint. The failure of the models to describe properly the left–right correlation becomes very clear in the case where it becomes very strong, due to near-degeneracy, in the near-dissociation

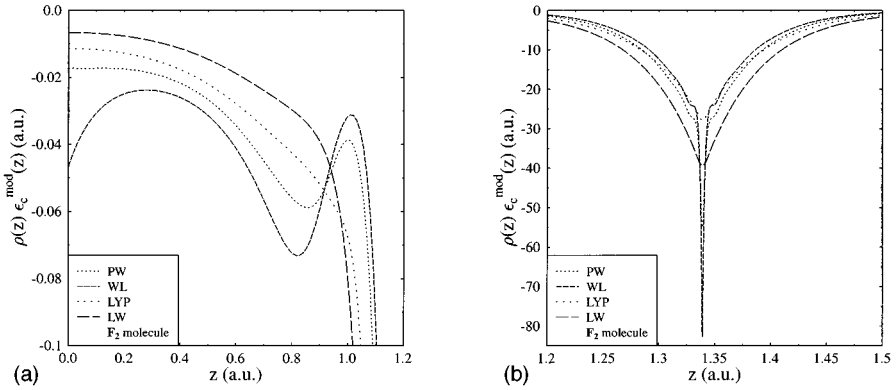

FIG. 5. Correlation energy densities $e_c^{\mathrm{mod}}(z)$ for F_2 in the bonding region (a) and in the atomic region (b). The bond midpoint is at $z=0$, the F nucleus is at $z=1.339$ a.u.

limit, $R(\mathrm{H}-\mathrm{H})=5.0$ a.u. [Fig. 4(b)]. In this case $e_c^{\mathrm{mod}}(z)$ have been calculated with ρ obtained with the CI, since the HF density (which we use to calculate e_c^{mod} in all other cases) differs substantially from the CI one for the dissociating H_2 molecule.[12] Figure 4(b) shows that the $e_c(z)$ obtained from the correlated $\rho(\mathbf{r}',\mathbf{r})$ and $\rho_2(\mathbf{r}_1,\mathbf{r}_2)$ possesses deep and wide wells around the nuclei. Contrary to this, all model functions exhibit much smaller wells around the nuclei. The model energy densities are completely determined by the electron density, which is practically the H atom density, and cannot recognize from this electron density the strong left–right correlation in the H_2 system with a concomitant deep Coulomb hole around the reference electron. They will in fact integrate to almost the same correlation energy (-0.03–-0.04 a.u.) as for the equilibrium H–H distance, whereas the exact e_c will integrate to -0.3125 a.u.[44] As a matter of fact, the gradient corrected density functionals for exchange deviate by approximately the same amount from the exact exchange [cf. second term in Eq. (11)], so that the total $E_{\mathrm{xc}}^{\mathrm{mod}}$ is fairly accurate. This compensation of ''errors'' in the correlation functionals by opposite errors in the exchange functionals seems to be fairly systematic, resulting in accurate total E_{xc} values from the existing gradient-corrected total functionals.

We note that the large peak in v_{kin} at the bond midpoint [Fig. 3(b)] is much diminished by the multiplication by the small $\rho(z)$ at the bond midpoint but it is still visible in a small positive value of e_c at $z=0$. The model e_c^{mod} are everywhere negative functions.

In order to examine if the observations made above apply to larger systems we briefly look at the $e_c^{\mathrm{mod}}(z)$ calculated for the Be_2 and F_2 molecules at their equilibrium bond distances. In Figs. 5(a) and 6(a) the model functions are plotted for the bonding regions only. Like H_2, F_2 is a molecule with a single covalent bond and for both molecules $e_c^{\mathrm{mod}}(z)$ have a similar form [compare Figs. 4(a) and 5(a)]. In particular, e_c^{WL} displays the same sharp minimum at $z=0$, while e_c^{PW}, e_c^{LYP}, and e_c^{LW} are rather shallow functions with maxima at $z=0$. A marked difference between $e_c^{\mathrm{mod}}(z)$ for H_2 and F_2 is the atomic shell structure of the gradient models e_c^{PW} and e_c^{WL} in the latter case, i.e., the additional nonmonotonous dependence of e_c^{mod} on z with extrema between the

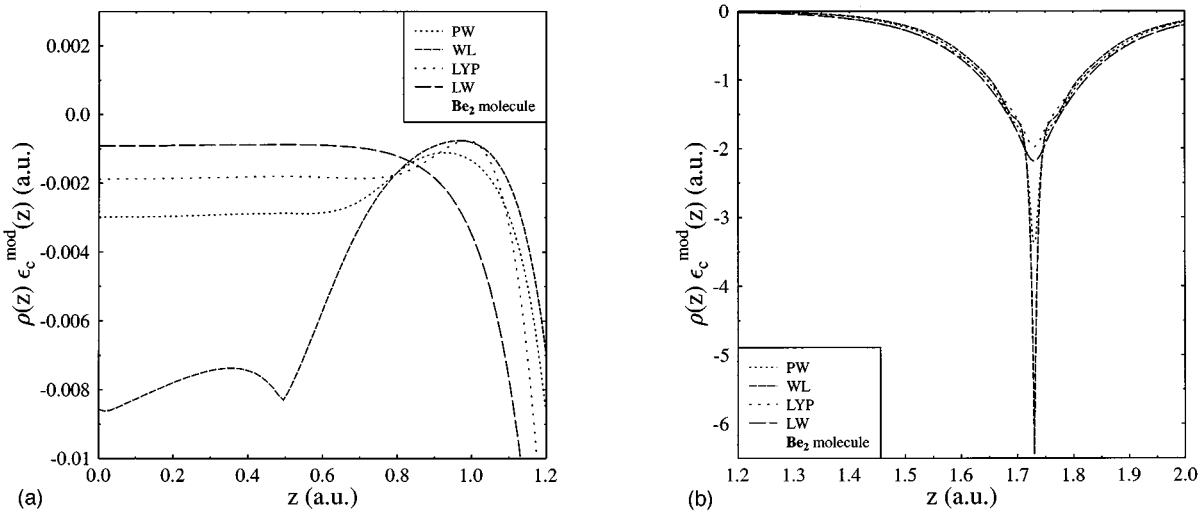

FIG. 6. Correlation energy densities $e_c^{\mathrm{mod}}(z)$ for Be_2 in the bond region (a) and in the atomic region (b). The bond midpoint is at $z=0$, the Be nucleus is at $z=1.730$ a.u.

TABLE II. Correlation energies of molecules obtained by various model correlation energy functionals. The notations of model functionals are the same as in Table I. EXP denotes the experimental correlation energies (Ref. 34). For CO and C_2H_4 the experimental correlation energies were estimated by using experimental atomization energies on the basis of the following reference: N. O. Oliphant and R. J. Bartlett, J. Chem. Phys. **100**, 6550 (1994). All the energies are in a.u. The calculations were performed using the large TZV+3D basis.

Molecule	WL	LYP	LW	PW	EXP
H_2	0.049	0.038	0.029	0.046	0.041
Li_2	0.136	0.133	0.134	0.137	0.122
Be_2	0.231	0.200	0.193	0.205	0.205
B_2	0.336	0.289	0.265	0.296	0.330
C_2	0.446	0.384	0.344	0.391	0.514
N_2	0.532	0.483	0.435	0.490	0.546
O_2	0.621	0.583	0.533	0.588	0.657
F_2	0.683	0.675	0.633	0.671	0.746
H_2O	0.386	0.340	0.314	0.347	0.367
NH_3	0.376	0.318	0.268	0.338	0.338
CH_4	0.369	0.294	0.241	0.320	0.293
HF	0.377	0.363	0.335	0.367	0.387
LiH	0.088	0.089	0.083	0.092	0.083
LiF	0.417	0.418	0.343	0.415	0.447
HCN	0.525	0.464	0.410	0.478	0.527
CO	0.516	0.484	0.440	0.488	0.550
H_2O_2	0.690	0.638	0.569	0.652	0.691
C_2H_2	0.504	0.443	0.386	0.466	0.476
C_2H_6	0.678	0.551	0.426	0.577	0.553
C_2H_4	0.593	0.497	0.417	0.529	0.528
CO_2	0.865	0.791	0.720	0.807	0.829

atomic shells [see Fig. 5(a)]. Since ρ itself is a monotonous function of z in atomic regions, the LW model does not display the atomic shell structure. It is interesting to note, however, that, in spite of its dependence on $|\nabla\rho(\mathbf{r})|$, the LYP model also does not show the shell structure in this case.

Unlike H_2 and F_2, Be_2 is a system with a weak bond with contributions from the interatomic correlation (dispersion forces) of electrons of two closed-shell Be atoms. Because of this, all $e_c^{\mathrm{mod}}(z)$ are close to zero in the bonding region of Be_2 [see Fig. 6(a); note the difference in scale with Fig. 6(b)]. In particular, e_c^{WL} displays its characteristic bond midpoint minimum but with very small depth and shallow form. e_c^{LYP} exhibits in this case atomic shell structure with a maximum at $z\approx 1$ a.u., while e_c^{PW} is a much more shallow function of z as compared to other gradient models.

Obviously, the differences amongst the model correlation energy densities are as large for these systems as they were found to be for H_2 and more work will be needed, including the calculation of accurate e_c, to clarify the topology of these energy densities.

Table II represents E_c values calculated for 21 closed-shell molecules with the PW, LYP, WL, and LW models. For H_2 the error compensation referred to above clearly is quite effective, the E_c values obtained from the model functionals all yielding a reasonable estimate of the experimental number. In fact, for all the molecules all functionals yield similar, reasonable, E_c values in spite of the considerable local differences between the energy densities. Considering the results more closely we note that the models produce appreciable deviations from the conventional empirical total E_c^e energies.[34] In quite a few cases for each functional these deviations exceed 0.05 a.u. The best results are obtained with the WL functional, in particular, for all dimers from B_2 to F_2 it provides the closest correspondence between the calculated and empirical E_c values. This fits with the results of Ref. 45, where better dissociation energies for dimers and monohydrides were obtained with the combination of the HF and WL functionals as compared to those obtained with the HF and PW functionals. Still, both PW and LYP models yield better E_c values than the WL ones for 8 out of 21 molecules. In particular, PW and LYP are better for H_2, Be_2, NH_3 and for all hydrocarbons considered (the only exception in the latter case is C_2H_2, for which WL yields a slightly better value than LYP; note that the triply bonded C_2H_2 is isoelectronic with N_2).

A possible explanation for this behaviour of the Wilson–Levy functional can be gleaned from Figs. 4–6, which demonstrate that there is a clear minimum in e_c^{WL} in the bond midpoint region. The WL model produces an extra contribution to E_c from this region. Since the values of the model energy densities e_c^{mod} are much lower in the bond region than in the atomic regions [cf. the different scales in Figs. 5(a) and 6(a) compared to Figs. 5(b) and 6(b)] it is not immediately obvious that the larger correlation energies for Wilson–Levy do indeed originate from the bond region. We have explicitly verified this by partitioning the molecular volume in various regions and considering the partial contributions. Taking for instance for F_2 for the bond region the disk $-1.0\leqslant z\leqslant +1.0$, this region accounts for ca. 20% of the total E_c, but its contribution already is more negative for Wilson–Levy compared to the other models by a larger amount than the total E_c is. So the atomic regions do give the largest contribution to E_c, but do not cause the more negative value of the Wilson–Levy E_c (actually they slightly counteract this effect of the bond region). This more negative bond region contribution of Wilson–Levy brings the E_c values closer to the ''experimental'' E_c^e and in this sense accounts effectively for the strong near-degeneracy correlation effects in dimers. Usually, $E_c[\rho]$ functionals derived from atomic data or from the electron gas model tend to underestimate correlation in dimers and this is true for the PW, LYP, and LW models (see Table II). Still, as has been pointed out above, the bond midpoint minimum of e_c^{WL} is an artificial topological feature of the WL functional, which will appear independently of the presence or absence of the strong near-degeneracy correlation effects. Due to this, the WL model overestimates E_c for hydrocarbons, for which the energetical effect of the near-degeneracy left–right correlation is not as strong as for multiply bonded dimers. It is also of course unsatisfactory that the bond midpoint behavior of the Wilson–Levy functional is opposite to the effect of strong left–right correlation as represented with the functions $\epsilon_c(\mathbf{r})$ and $e_c(\mathbf{r})$ obtained from the correlated $\rho(\mathbf{r}',\mathbf{r})$ and $\rho_2(\mathbf{r}_1,\mathbf{r}_2)$. One can see from Figs. 3 and 4 that correlation produces a maximum (and not minimum) in the bond midpoint region.

VI. CONCLUSIONS

In this paper it has been proposed to construct the exchange-correlation and correlation energy densities from

the first- and second-order correlated density matrices obtained with *ab initio* calculations. The functions $\epsilon_c(\mathbf{r})$ as well as their kinetic $v_{\mathrm{kin}}(\mathbf{r})$ and potential $(1/2)w_c(\mathbf{r})$ components have been presented for the two-electron He atom and H_2 molecule. A manifestation of various correlation effects through the form of these functions has been discussed. The corresponding functions $e_c(\mathbf{r})$ have been compared with $e_c^{\mathrm{mod}}(\mathbf{r})$ of some local and gradient approximations. The model energy densities $e_c^{\mathrm{mod}}(\mathbf{r})$ have been compared also for the Be_2 and F_2 molecules and E_c values have been calculated for a number of atoms and molecules.

The present results show that, in spite of some success of the gradient models, further improvement of the DFT approximations to $e_c(\mathbf{r})$ is desirable, especially, to describe properly the correlation in molecular systems. The errors of the GGA correlation functionals in molecules with strong near-degeneracy correlation seem to be compensated systematically by opposite errors in the GGA exchange functionals (either Becke[46] or Perdew–Wang[6]), explaining the success of the molecular applications of the generalized gradient approximation (GGA) reported recently.[6,47] In those cases a combined treatment of exchange and correlation may be more useful.

As for correlation models, the functions $\epsilon_c(\mathbf{r})$ obtained from the correlated $\rho(\mathbf{r}',\mathbf{r})$ and $\rho_2(\mathbf{r}_1,\mathbf{r}_2)$ can serve as a benchmark for successful models $e_c^{\mathrm{mod}}(\mathbf{r})$. The procedure presented in Sec. II allows to construct $\epsilon_c(\mathbf{r})$ and $e_c(\mathbf{r})$ for an arbitrary many-electron system, which opens new possibilities for the DFT modeling. When developing a new $\epsilon_c^{\mathrm{mod}}(\mathbf{r})$, one can take into account not only E_c estimates or the scaling and asymptotic properties of the E_c functional, but also the local behavior of the essentially accurate $\epsilon_c(\mathbf{r})$ obtained from *ab initio* wave functions for a representative set of atomic and molecular systems. A promising option is to approximate directly the potential $(1/2)w_c(\mathbf{r})$ and kinetic $v_{\mathrm{kin}}(\mathbf{r})$ components which, as has been shown in the present paper, have a characteristic form. The corresponding work as well as the application of the proposed procedure of $\epsilon_c(\mathbf{r})$ construction to systems with more than two electrons is in progress.

ACKNOWLEDGMENTS

We gratefully acknowledge funding by the Netherlands Foundation for Scientific Research (NWO) and the Stichting Fundamenteel Onderzoek der Materie (FOM). This work has been sponsored by the Hungarian–U.S. Science and Technology Joint Fund in cooperation with the National Science Foundation and Hungarian Academy of Sciences under Project 146/91. It has also been supported by the Grant OTKA Nos. TO16621 and TO16623, by the European Mobility Scheme for Physics Students (EMSPS) as part of the TEMPUS grant.

[1] R. G. Parr and W. Yang, *Density Functional Theory of Atoms and Molecules* (Oxford University, Oxford, 1989).
[2] R. M. Dreizler and E. K. U. Gross, *Density Functional Theory: An Approach to the Quantum Many-Body Problem* (Springer, Berlin, 1990).
[3] *Theory of the Inhomogeneous Electron Gas*, edited by S. Lundqvist and N. H. March (Plenum, New York, 1983).
[4] J. P. Perdew, in *Electronic Structure of Solids '91* (Akademie, Berlin, 1991).
[5] Yue Wang and J. P. Perdew, Phys. Rev. B **44**, 13298 (1991).
[6] J. P. Perdew, J. A. Chevary, S. H. Vosko, K. A. Jackson, M. R. Pederson, D. J. Singh, and C. Fiolhais, Phys. Rev. B **46**, 6671 (1992).
[7] C. Lee, W. Yang, and R. G. Parr, Phys. Rev. B **37**, 785 (1988).
[8] L. C. Wilson and M. Levy, Phys. Rev. B **41**, 12930 (1990).
[9] P. Gombás, *Pseudopotential* (Springer, Berlin, 1967).
[10] J. P. Perdew and Yue Wang, Phys. Rev. B **45**, 13244 (1992).
[11] O. V. Gritsenko, R. van Leeuwen, and E. J. Baerends, J. Chem. Phys. **101**, 8955 (1994).
[12] M. A. Buijse, E. J. Baerends, and J. G. Snijders, Phys. Rev. A **40**, 4190 (1989).
[13] G. Hunter, Int. J. Quantum Chem. **29**, 197 (1986).
[14] O. Gunnarson and B. I. Lundqvist, Phys. Rev. B **13**, 4274 (1976).
[15] D. C. Langreth and J. P. Perdew, Solid State Commun. **17**, 1425 (1975).
[16] Y. Wang and R. G. Parr, Phys. Rev. A **47**, R1591 (1993).
[17] R. van Leeuwen and E. J. Baerends, Phys. Rev. A **49**, 2421 (1994).
[18] Q. Zhao, R. C. Morrison, and R. G. Parr, Phys. Rev. A **50**, 2138 (1994).
[19] S. H. Werden and E. R. Davidson, in *Local Density Approximations in Quantum Chemistry and Solid State Physics* (Plenum, New York, 1982).
[20] C. O. Almbladh and A. C. Pedroza, Phys. Rev. A **29**, 2322 (1984).
[21] F. Aryasetiawan and M. J. Stott, Phys. Rev. B **38**, 2974 (1988).
[22] Á. Nagy and N. H. March, Phys. Rev. A **39**, 5512 (1989).
[23] A. G. Görling, Phys. Rev. A **46**, 3753 (1992).
[24] O. V. Gritsenko, R. van Leeuwen, and E. J. Baerends, Phys. Rev. A **52**, 1870 (1995).
[25] M. A. Buijse, Ph.D. thesis, Vrije Universiteit, Amsterdam, The Netherlands, 1991.
[26] J. D. Doll and W. P. Reinhardt, J. Chem. Phys. **57**, 1169 (1972).
[27] G. C. Lie and E. Clementi, J. Chem. Phys. **60**, 1275 (1974).
[28] R. Poirier, R. Kari, and I. G. Csizmadia, *Handbook of Gaussian Basis Sets* (Elsevier, Amsterdam, 1985).
[29] V. R. Saunders and J. H. van Lenthe, Mol. Phys. **48**, 923 (1983).
[30] E. P. Wigner, Trans. Faraday Soc. **34**, 678 (1938).
[31] M. Gell-Mann and K. A. Brueckner, Phys. Rev. **106**, 364 (1957).
[32] G. Brual and S. M. Rothstein, J. Chem. Phys. **69**, 1177 (1978).
[33] P. Süle and Á. Nagy, Acta Phys. Chim. Debr. **29**, 1 (1994).
[34] A. Savin, H. Stoll, and H. Preuss, Theoret. Chim. Acta **70**, 407 (1986).
[35] M. Levy and J. P. Perdew Phys. Rev. A **32**, 2010 (1985).
[36] R. Colle and D. Salvetti, Theoret. Chim. Acta **37**, 329 (1975).
[37] B. Miehlich, A. Savin, H. Stoll, and H. Preuss, Chem. Phys. Lett. **157**, 200 (1989).
[38] M. Buijse and E. J. Baerends, in *Density Functional Theory of Molecules, Clusters and Solids*, edited by D. E. Ellis (Kluwer, Amsterdam, 1995).
[39] M. W. Schmidt and K. K. Balchidge, J. Comput. Chem. **14**, 1347 (1993).
[40] T. Dunning, J. Chem. Phys. **55**, 716 (1971).
[41] T. Dunning, J. Chem. Phys. **55**, 3958 (1971).
[42] E. Clementi, S. J. Chakravorty, G. Corongiu, and V. Carravetta, in MOTECC-89.
[43] H. Stoll, C. M. E. Pavlidou, and H. Preuss, Theoret. Chim. Acta **49**, 143 (1978).
[44] R. van Leeuwen, Ph.D. thesis, Vrije Universiteit, Amsterdam, The Netherlands, 1994.
[45] P. Fuentealba and A. Savin, Chem. Phys. Lett. **217**, 566 (1994).
[46] A. D. Becke, Phys. Rev. A **38**, 3098 (1988).
[47] A. D. Becke, J. Chem. Phys. **97**, 9173 (1993).